Ion Mobility of Precritical Clusters in Supersaturated Vapors: Condensation of Supersaturated Methanol Vapor Induced by Toluene and Styrene Ions

ARTICLE *in* THE JOURNAL OF PHYSICAL CHEMISTRY A · JUNE 2000

Impact Factor: 2.69 · DOI: 10.1021/jp991934g

4 AUTHORS, INCLUDING:

Sergey Fisenko
National Academy of Sciences of Belarus
143 PUBLICATIONS **607** CITATIONS
SEE PROFILE

M. Samy El-Shall
Virginia Commonwealth University
272 PUBLICATIONS **4,575** CITATIONS
SEE PROFILE

Ion Mobility of Precritical Clusters in Supersaturated Vapors: Condensation of Supersaturated Methanol Vapor Induced by Toluene and Styrene Ions

D. Kane,[†] M. Rusyniak, S. P. Fisenko,[‡] and M. S. El-Shall*

Department of Chemistry, Virginia Commonwealth University, Richmond, Virginia 23284-2006

Received: June 11, 1999; In Final Form: February 24, 2000

A new method for measuring the ion mobility of precritical clusters in supersaturated vapors is reported. The method is based on the REMPI (Resonance Enhanced Multiphoton Ionization) nucleation technique, which allows the generation of selected ions within a supersaturated host vapor held in a diffusion cloud chamber. The precritical cluster ions drift under the influence of a uniform electric field to the nucleation zone, where they become condensation nuclei and rapidly grow into macroscopic liquid droplets that can be detected by light scattering. The reduced mobility of the precritical clusters in the toluene$^+$/methanol and styrene$^+$/methanol systems decreases with increasing methanol supersaturation, which reflects the increase in the size of the solvated ion in agreement with Thomson's model for ion-induced nucleation.

1. Introduction

Although nucleation is one of the most ubiquitous and important phenomenon in science and technology, the nucleus for condensation remains one of the most elusive entities known in chemical physics and has never been observed directly.[1−6] Only the consequences of its presence, e.g., droplet formation, precipitation, and so forth, are observed. For example, in vapor phase nucleation studies, the nucleation rate is often obtained by measuring the rate of production of macroscopic liquid droplets from the vapor phase. In ion-induced nucleation studies, the problem is further complicated by the unknown identity of the nucleating ions responsible for initiating the condensation of the vapor.[7−13]

Ion-induced nucleation is a phenomenon of great importance not only as a subject for basic scientific inquiries of complex phenomena in chemical physics but also for many atmospheric, environmental, and industrial implications. Detailed knowledge of ion nucleation in the vapor phase is crucial for the understanding of many important problems, such as chemical reactions in the ionosphere, condensation of interstellar dust, formation of acid rain and environmental pollutants, and for other applications in radiation chemistry and combustion processes.

Although many powerful techniques based on mass spectrometric detection have been developed to study the properties of cluster ions, most of these techniques are inappropriate for studying the mechanism of ion-induced nucleation.[14−17] The problem is rooted in the fact that well-defined nucleation parameters, such as the temperature and supersaturation of the condensing vapor, are almost impossible to obtain under typical mass spectrometric conditions, at which the vapor phase is essentially absent during the detection of the cluster ions. One obvious approach to overcome this problem is to develop new techniques that combine the well-defined nucleation parameters characteristic of established nucleation devices, such as cloud chambers, with mass spectrometric techniques to identify the cluster ions involved in the nucleation process. However, many questions and concerns relating to the sampling process need to be resolved before such a strategy can be adopted to obtain a molecular-level understanding of the ion-induced nucleation phenomenon.

A complete understanding of the role of various molecular properties in ion-induced nucleation is necessary for the development of proper molecular theories for nucleation, with the implicit assumption that these theories will provide a better picture of how ion−molecule and intermolecular interactions lead to the rich dynamic behavior of condensed phase systems. Because different ionic species are characterized by different mobility, it is almost impossible to obtain accurate quantitative data on ion nucleation without identifying the nucleating ions. This is because more mobile ions could be easily removed from the nucleation zone under the influence of the applied electric field.

The first experiment that unambiguously identified the nature of the nucleating ions has only been reported in 1995, when we demonstrated the first application of REMPI (Resonant Enhanced Multiphoton Ionization) to selectively generate molecular ions within a supersaturated host vapor.[18−23] REMPI results when the energy of one or more of the incident photons matches that of an intermediate state of the selected chromophore molecule, thus resulting in strong enhancement of the multiphoton ionization probability produced by tuning into resonance at the energy of the intermediate state.[24] This highly sensitive spectroscopic technique allows selected molecules to be ionized in a mixture, whereas the other components remain transparent to the ionizing radiation. It is also one of the most rigorously fragmentation-free methods of preparing molecular ions.[24] The advantages of REMPI as a spectroscopic and analytical ionization technique when combined with the amplification and detection capabilities of nucleation and growth provide ideal environments for detailed studies of ion nucleation, as well as a wide variety of other chemical physical phenomena, including analytical applications.

Our approach is based on the selective ionization by REMPI of a chromophore molecule present at a trace concentration within a supersaturated host vapor.[18,19] The experiment uses a diffusion cloud chamber (DCC) to produce a steady-state supersaturated vapor. Selected ions generated within the supersaturated vapor cluster with the vapor molecules forming

* To whom correspondence should be addressed. E-mail: selshall@hsc.vcu.edu.

[†] Current address: Department of Chemistry, University of Delaware, Newark, Delaware, 19716.

[‡] Permanent address: A. V. Luikov Heat and Mass Transfer Institute, Academy of Sciences of Belarus, Minsk, Belarus.

10.1021/jp991934g CCC: $19.00
Published on Web 05/06/2000

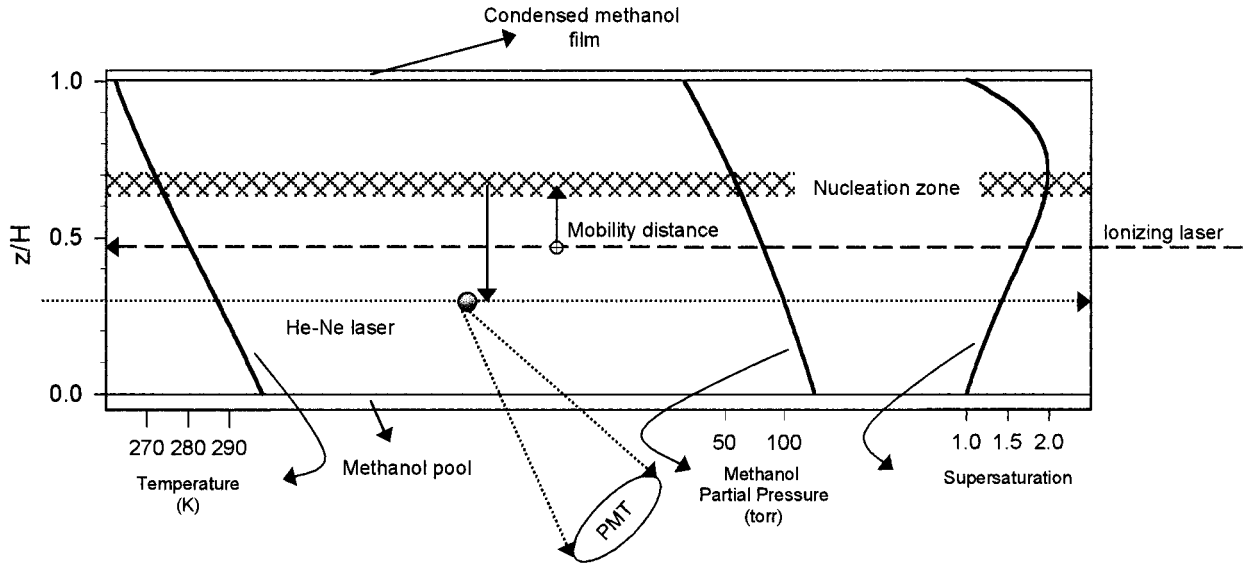

Figure 1. Schematic of the REMPI-nucleation experiment showing typical temperature, partial pressure, and supersaturation profiles for the ion-induced nucleation of supersaturated methanol vapor by toluene ions.

condensation nuclei, which rapidly grow to macroscopic liquid droplets that can be detected by light scattering. The method has tremendous amplification and detection capabilities and is expected to provide a valuable new analytical tool for the identification of trace components in the vapor phase.[18−23]

In this paper, we report a new application of the REMPI nucleation technique for the measurement of the mobility of precritical cluster ions in supersaturated vapors under well-defined nucleation conditions. Ion mobility is becoming an increasingly important tool for the determination of the structures and conformations of molecular and cluster ions as well as for the thermochemistry and kinetics of ion−molecule reactions.[16,17,25−28] However, no studies have been reported on cluster ions involved in a typical vapor phase nucleation process.

The approach used in the present study can be described as follows: Toluene or styrene molecular ions are generated by REMPI within a supersaturated methanol vapor held in a thermal DCC. The DCC is operated as a drift cell by applying a uniform electric field across the bottom and top plates of the chamber. The ions are generated below the maximum supersaturation region of the chamber; methanol molecules cluster around the ions, and the cluster ions drift under the influence of the uniform field toward the nucleation zone (maximum supersaturation region) where nucleation occurs. The resulting condensation nuclei rapidly grow into macroscopic liquid droplets (several microns in diameter), and the droplets fall by gravity into a He−Ne laser beam. The light signals scattered by the droplets are detected by a photomultiplier and recorded using a computer interface. The arrival time distribution (ATD) is measured as a function of the drift field across the chamber. The data are used to calculate the mobility of the cluster ions, and from the dependence of the measured mobility on the vapor supersaturation, we can relate the size distribution of the precritical cluster ions to the nucleation parameters. Note that the experiment allows in situ detection of the nucleating ions and no mass spectrometric sampling is required. We also note that these experiments provide direct evidence for the presence of precritical clusters in supersaturated vapors, which lead to the formation of condensation nuclei. In particular, we provide the first direct experimental evidence for increasing the size of the precritical cluster ions by increasing the vapor supersaturation, as predicted by Thomson's model for ion-induced nucleation.[29]

The outline of the paper is as follows: In the Experimental Section, we describe the experimental method used to measure the mobility of the cluster ions in supersaturated vapors. In the results and discussion section, we present the results for the toluene and styrene ions in supersaturated methanol vapor. We also present the calculation of the ion distribution in the nucleation zone and show that the experimental time profiles can be simulated using the calculated ion distribution. Finally, we compare the trends observed experimentally with the predictions of Thomson's model for ion-induced nucleation.

2. Experimental Section

The experimental setup for the REMPI nucleation studies is shown schematically in Figure 1. It consists of three major components: an upward thermal DCC that is used to produce the supersaturated host vapor, a tunable UV laser system for the generation of the selected ions by REMPI, and a light scattering detection system consisting of an He−Ne laser, photomultiplier, and a computer interface for measuring the scattered light from the nucleating droplets.

The DCC consists of two metal plates separated by a glass ring.[30,31] A shallow pool of the condensing liquid (methanol in the present experiments) rests on the bottom surface of the chamber, and the remainder of the chamber is filled with He (99.999% pure) at a total pressure of 300−500 Torr. The methanol pool contains 0.000 05 mole fraction of the chromophore to be resonantly ionized, either toluene or styrene in the present study. A supersaturated vapor is established in the chamber by heating the lower surface and cooling the upper surface. This causes molecules to evaporate from the liquid pool, diffuse through the He carrier gas, and condense on the top plate. The DCC has been carefully designed so that the diffusion process within the chamber is highly one-dimensional.[30,31] This makes it possible to accurately determine the thermodynamic state in the chamber by solving the boundary value problem associated with the heat and mass flux within the chamber.[30,31] A profile of the temperature, partial pressure of the vapor, and supersaturation inside the chamber is shown in Figure 1. The temperature in the chamber falls off linearly with the height. The density and vapor partial pressure falls off nearly linearly as well. Because the equilibrium vapor pressure is an exponential function of temperature, it decreases much faster than the partial

pressure of the vapor. Therefore, everywhere in the chamber, except at the top and bottom surfaces where vapor−liquid interfaces exist, the vapor is supersaturated. In the DCC, the supersaturation reaches a maximum, at about 75% of the height of the chamber. Because of the temperature and supersaturation dependence of the nucleation rate, nucleation will only occur in a narrow region within the chamber height, called the nucleation zone, which is located slightly below the maximum supersaturation in the DCC.[12,22] Increasing the temperature gradient between the top and bottom surfaces of the chamber can increase the vapor supersaturation in the chamber to the critical supersaturation for homogeneous nucleation and beyond.

The tunable UV radiation is provided by an excimer-pumped dye laser combination (Lambda Physik LPX 101/FL3002) with the output passing through a β-BaB_2O_4 crystal cut at 52° to generate the second harmonic of the dye laser output pulse. The toluene and styrene molecular ions are generated by the two-photon absorption at the corresponding 0^0_0 transitions at 37 482 and 34 760 cm^{-1}, respectively.[32,33] With the chamber set to a temperature gradient below the threshold for homogeneous nucleation, ions are produced in the chamber by a single, 10 ns, ∼60 μJ laser pulse. The ionizing laser pulse enters the chamber through quartz windows in the glass ring of the chamber. The laser pulse passes through the center of the chamber at a reduced height, (z/H, where H, the total chamber height, is 5.1 cm) of 0.5.

Because of the exponential dependence of the nucleation rate on the vapor supersaturation,[1−6] when ions are formed in the chamber they must first travel to the nucleation zone, where, if the supersaturation is large enough, nucleation will occur. The resulting nuclei grow rapidly to form macroscopic droplets. The droplets are observed to occur in a narrow plume along the path of the ionizing laser pulse. Under typical experimental conditions, between few to several hundred droplets result from a single laser pulse, growing to macroscopic size and falling back to the liquid pool within several hundred milliseconds. The He−Ne laser beam is directed below and parallel to the path of the ionizing laser pulse (z/H = 0.3−0.4). A photomultiplier positioned to detect the forward-scattered light is used to measure the intensity of the nucleation signal. The signal from the photomultiplier is sampled as a function of time at 10 000 Hz by an analogue to digital converter and recorded by a computer.

The arrival time distribution (ATD) for ion-induced nucleation is defined as the time elapsed between the creation of the ions and the arrival of the droplets at the detector. In the present experiments, the ATD is taken as the time period between the firing of the ionizing laser and the time of the maximum intensity in the scattered light peak. It has previously been determined that the maximum intensity of the scattered light corresponds to droplets falling from the maximum rate plane in the DCC, i.e., the center of the nucleation zone. It should be noted that the ATD includes the time for ionization (∼10^{-8} s), the time for the ions to travel to the nucleation zone (∼10^{-2} − 10^{-3} s), the time for nucleation (∼10^{-6} s), and the time for the droplets to grow and fall to the detector (∼0.3−0.4 s).

3. Results and Discussion

A. Measurement of the Ion Mobility of the Precritical Clusters. Figure 2a displays the nucleation spectrum obtained from the DCC experiment of toluene-doped methanol vapor. The nucleation spectrum is obtained by measuring the total droplet count (TDC) obtained following a single dye laser pulse of a given frequency. The spectrum shown in Figure 2a was

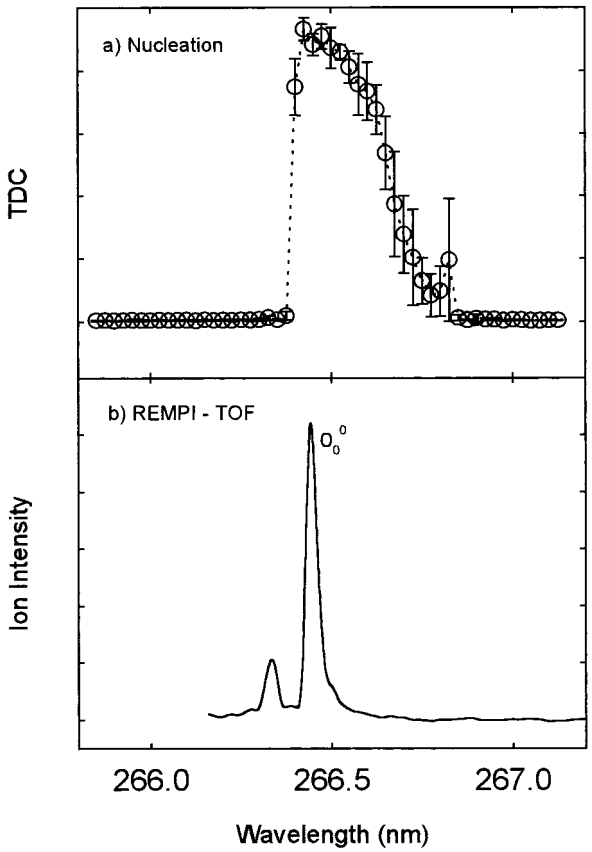

Figure 2. (a) Nucleation spectrum of supersaturated methanol vapor induced by the REMPI of toluene through the 0^0_0 transition. Maximum supersaturation = 1.33 at T = 283.9 K and total pressure in He = 586 Torr. (b) REMPI-TOF spectrum in the vicinity of the 0^0_0 transition of toluene in a molecular beam.

obtained by averaging the TDC obtained from five individual dye laser pulses. The sharp increase in the TDC at the frequency corresponding to the 0^0_0 transition of toluene is clearly evident in Figure 2a.

Figure 2b exhibits the 0^0_0 REMPI-TOF spectrum of toluene obtained in a molecular beam coupled with a time-of-flight (TOF) mass spectrometer.[34] The jet cooled REMPI spectrum reflects the freezing of many degrees of freedom, as compared to the REMPI-nucleation spectrum obtained at T = 283.9 K. However, the remarkable similarity between the TOF and nucleation spectra provides strong evidence that the supersaturated methanol vapor is condensing on the toluene molecular ions. Similarly, in the styrene$^+$/methanol experiments, ion-induced nucleation is observed only in the vicinity of the 0^0_0 transition of styrene (34 760 cm^{-1}).

The average velocity of the ions, v, travelling toward the nucleation zone in the DCC under the influence of a homogeneous electric field is given by[35]

$$v = KE \tag{1}$$

where K is the ion mobility, and E is the electric field. Figures 3 and 4 display the ATD at different electric fields for the ion-induced nucleation of methanol on toluene and styrene ions, respectively. It is evident that the ATD is affected by the electric field across the DCC. It is clear that as the field is increased the width of the nucleation peak decreases, and the ATD decreases. Also, we note that TDC, defined as the integrated intensity over the ATD of the droplets, is inversely proportional to the electric field.

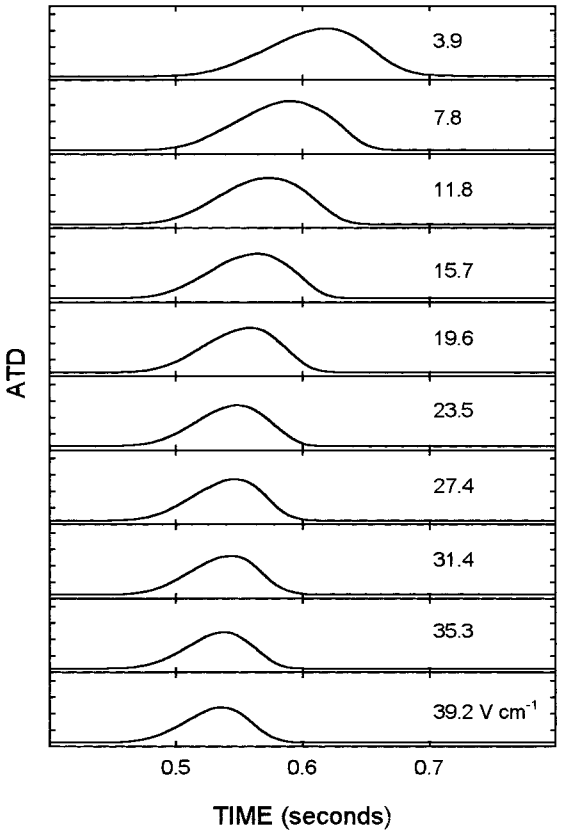

Figure 3. Arrival time distribution (ATD) of the methanol droplets following the 0^0_0 REMPI of toluene at different electric fields applied between the chamber plates. Chamber conditions for this experiment were $P_{tot} = 302$ Torr, $T_0 = 298$ K, and $T_1 = 262$ K.

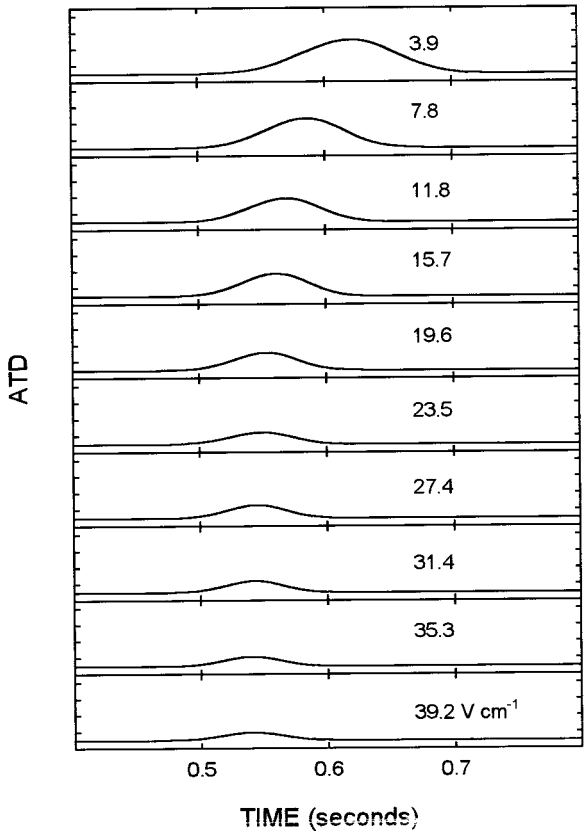

Figure 4. Arrival time distribution (ATD) of the methanol droplets following the 0^0_0 REMPI of styrene at different electric fields applied between the chamber plates. Chamber conditions for this experiment were $P_{tot} = 400$ Torr, $T_0 = 302$ K, and $T_1 = 267$ K.

The ATD depends on the times of ionization, ion motion, nucleation, and droplet growth. The two major contributions to the ATD arise from the drift time of the ions travelling to the nucleation zone and the time for the nucleating droplets to grow and fall to the detector. Calculations using a model for droplet growth and motion, described in reference 22, show that the range of fields used in the present experiments has a negligible effect on the falling time of the droplets (the electric field will tend to slightly increase, not decrease, the falling time for the droplets as it acts in the opposite direction of the gravity field). This indicates that the change in the time profiles with the electric field is primarily due to the change in the distribution of the ion cloud in the DCC, as a result of the applied electric field (see Section B). Therefore, the ATD can be approximated as

$$\mathrm{ATD} = t_{\mathrm{fall}} + t_{\mathrm{d}} = t_{\mathrm{fall}} + \frac{L}{KE} \tag{2}$$

where t_{fall} is the time for the droplets to grow and fall to the He−Ne laser beam, and t_{d} is the drift time for the ions to travel to the nucleation zone. L is the distance from the ionization region to the nucleation zone. Figures 5 and 6 display the ATD vs $1/E$ plots measured at different supersaturations for the toluene$^+$/methanol and styrene$^+$/methanol systems, respectively. From the slope of the ATD vs $1/E$ plot, we calculate the mobility K, which is then converted into reduced mobility K_0 according to the formula[35]

$$K_0 = \frac{P}{760}\frac{273.16}{T}K \tag{3}$$

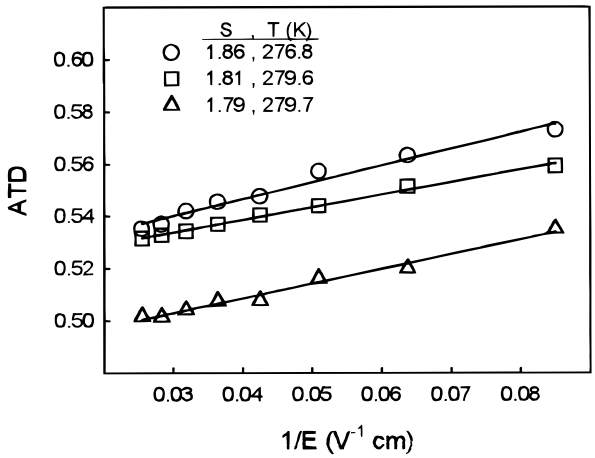

Figure 5. Plots of ATD vs $1/E$ (electric field) for the REMPI-induced nucleation of supersaturated methanol vapor by toluene ions at different supersaturations as indicated.

where the total pressure P is measured in Torr, and the temperature T is measured in Kelvin. The experimental conditions used to obtain the mobility data correspond to a characteristic parameter E/N (electric field/number density of the vapor expressed in 10^{-17} Vcm^2 = 1 Td) in the range 0.1−0.4 Td. This is well within the low field regime because $E/N < 6.0$ is generally considered to be in the low field region.[35]

The data shown in Figure 5 results in average reduced mobility of 0.61, 0.80, and 1.0 cm^2/Vs for the toluene$^+$-(methanol)$_n$ precritical clusters at the average methanol supersaturations of 1.86, 1.81, and 1.79 corresponding to average temperatures of 276.8, 279.6, and 279.7 K, respectively. Figure

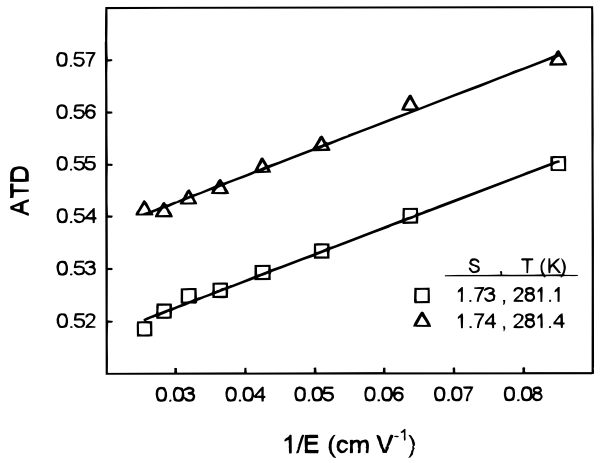

Figure 6. Plots of ATD vs 1/*E* (electric field) for the REMPI-induced nucleation of supersaturated methanol vapor by styrene ions at the same supersaturation but different values of applied fields.

6 demonstrates the reproducibility of the measured mobility at a given supersaturation using two different sets of applied fields. Both sets of data result in a reduced mobility of 1.0 cm^2/Vs for the styrene$^+$(methanol)$_n$ precritical clusters at the average methanol supersaturations of 1.73 and 1.74, corresponding to average temperatures of 281.1 and 281.4 K, respectively. Measurements at a supersaturation of 1.82 and a temperature of 277.6 K result in a reduced mobility of 0.14 cm^2/Vs. The average supersaturation and temperature are calculated from the chamber profiles over the region that the cluster ions travel (see Figure 1).

It should be noted that the resulting mobility is averaged over the cluster size range *n*, which depends on the methanol supersaturation. It is clear that the measured reduced mobilities are smaller than expected for the mobility of toluene or styrene ions moving through He. For example, the reduced mobility of toluene in air has been measured to be 1.87 cm^2/Vs.[36] In He, which is smaller and less polarizable than N_2, the toluene ions are expected to be more mobile.[37] Also, because of the similar sizes of toluene and styrene ions, their mobilities are expected to be similar. Therefore, it appears that the difference between the measured averaged mobilities of the toluene$^+$(methanol)$_n$ and styrene$^+$(methanol)$_m$ precritical clusters is due to different cluster distributions *n* and *m*.

The small mobility of the precritical toluene$^+$(methanol)$_n$ and styrene$^+$(methanol)$_n$ is consistent with the rapid clustering of the methanol molecules around the toluene or the styrene ions following the generation of the molecular ions. The decrease in mobility with increasing vapor supersaturation is only observed at higher values of supersaturation (about 95% of the critical supersaturation required for homogeneous nucleation rate of one drop/cm^3/s at a given temperature). In experiments with lower supersaturations, no apparent change of mobility with supersaturation is observed.[38] This indicates that very little or no clustering of the vapor molecules occurs around the solvated ions under low supersaturation conditions. In this case, the measured mobility reflects the mobility of the solvated ions formed initially after the generation of the selected ions in the supersatuated vapor.

B. Ion Distribution in the Nucleation Zone. In the REMPI nucleation experiments, the ions are created along the path of the UV laser pulse, which is roughly a cylindrical shape with the long axis parallel to the $x-y$ plane, the plane of the liquid surface at the top or bottom plate of the chamber. The relative contributions to the overall ion motion from drift velocity and diffusion depend on the geometry of the ion source, the applied voltage and the travel distance to nucleation zone. It is important to emphasize that the interpretation of the ion-induced nucleation experiments strongly depends on these parameters, which must be taken into consideration in the analysis of the results.

We consider the ion motion under the constant electric field along the *z*-axis. The ion density is denoted as n (z,r,t) and cylindrical symmetry of ion distribution about its center of mass is assumed as shown below.

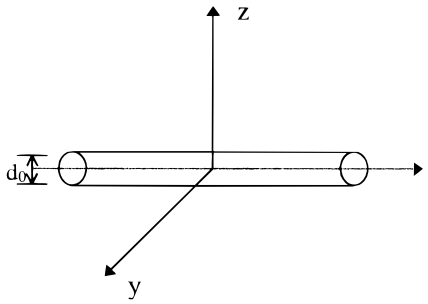

The initial ion distribution, n_0, is taken to be uniform in a cylindrical tube with diameter, d_0, which corresponds to the average diameter of the laser pulse in the DCC. The equation of motion for the ion distribution in the DCC is given by eq 4[39]

$$\partial_t n(z,r,t) = -v\partial_z n(z,r,t) + D\Delta n(z,r,t) \tag{4}$$

where Δ is the Laplacian in cylindrical coordinates, v is the drift velocity, and D is the diffusion coefficient. The ion velocity is related to the mobility by eq 1. However, diffusion causes the ions to spread out as they travel through the DCC. Under low field conditions, the diffusion coefficient D is related to the mobility by Einstein's relation[35]

$$D = Kk_BT/e \tag{5}$$

where e is the electron charge, and k_B is the Boltzmann constant.

The boundary conditions to eq 4 are n (z,r,t) = 0, where $r \gg d_0$, and the initial value of the ion distribution is described by the function n (z,r,0) = n_0 (z), and $n_0(z)$ equals to n_0 in the ionization volume and 0 outside.

The ion density in the nucleation zone can be estimated as follows: Because the time required for the center of mass of the ion cloud to travel a distance L is given by v/L, it is possible to estimate the expansion of the ion cloud because of ion diffusion after it has traveled a distance L. It is well known that the diffusion broadening during time t can be approximated as $\Delta \approx \sqrt{Dt}$.[39] For the cylindrical symmetry considered here, the diameter of the ion cloud as a function of the travelling distance L, i.e., $d(L)$, can be estimated as

$$d(L) \approx \sqrt{\frac{D\mu_0^2 L}{v}} = \sqrt{\frac{kT\mu_0^2 L}{Ee}} \tag{6}$$

where $\mu_0 \approx 2.4$ is the first root of the Bessel function of zero order. It follows from eq 5 and the law of conservation of charge that the average ion density $\langle n(L)\rangle$ will change with the distance L according to

$$\langle n(L)\rangle \approx n_0 \frac{d_0^2}{d(L)^2} = n_0 d_0^2 \frac{Ee}{kT\mu_0^2 L} \tag{7}$$

It is clear from (7), that the average density of the ion "cloud"

is directly proportional the strength of electric field and inversely proportional to the travelling distance L.

The analytical solution of eq 4 can be found following the transformation into a moving coordinate system centered on the ion cloud with velocity v. In this case, eq 4 transforms into the diffusion equation that describes pure radial diffusion

$$\partial_t n(r,t) = D\Delta n(r,t) \tag{8}$$

The position of the center of the ion cloud along z-axis can be written as

$$z(t) = z_0 + vt \tag{9}$$

where z_0 is the initial position.

The solution of diffusion equation can be written by means of a series of Bessel functions according to[40]

$$n(r,t) = \sum_{s=1}^{\infty} A_s J_0\left(\frac{\mu_s r}{b}\right)\exp\left(-\frac{D\mu_s^2 t}{b^2}\right) \tag{10}$$

where J_0 is the zeroth order Bessel function and μ_s is s^{th} root of the equation

$$J_0(x) = 0 \tag{11}$$

The expression for A_s is given by

$$A_s = \frac{2}{b^2 J_1^2(\mu_s)}\int_0^b r J_0\left(\frac{\mu_s r}{b}\right)dr \tag{12}$$

where J_1 is the first-order Bessel function.

In our numerical calculation, we take $b = 7d_0$, so $r \le b$ in order replace the boundary condition at infinity with the domain of finite size with quite high accuracy. It can be shown from the solution of eq 10, eq 5, and expression 6 that ion diffusion can be neglected if the distance (L) between the ionizing laser path and the plane of maximum nucleation rate (the saddle point of the free energy surface in the DCC[22]) satisfies the inequality

$$\frac{2.4^2 DL}{vb^2} = \frac{0.12Lk_B TH}{eU d_0^2} < 1 \tag{13}$$

where U is potential difference and H is the distance between the chamber plates. For this reason, only potentials (U) above 50 V were used in the determination of the ion mobility of the precritical clusters. It is interesting to note that condition 13 does not depend on the mobility of the precritical cluster ions but depends on the initial ion cloud diameter (d_0), the travel distance (L) and the temperature (T). Because $E = U/H$, it is evident that the parameter E/LT plays an important role in the ion nucleation experiments in the DCC.

Equation 4 was solved analytically with the approximation that the ion velocity is constant under the uniform electric field. The measured value of ion mobility for the toluene−methanol positive ion system and the distance for the ions to travel from the laser beam to the nucleation zone (L) were used in the numerical calculation. The dependence of initial number of ions created by REMPI on applied field was taken into account by calculating the degree of recombination from equations (4) and (7) in ref 21, with the recombination coefficient equal to 10^{-10}. Using the solution of the series (10), including 20 terms, the temporal profile of the ion density at the plane of maximum nucleation rate was calculated as a function of the applied field.

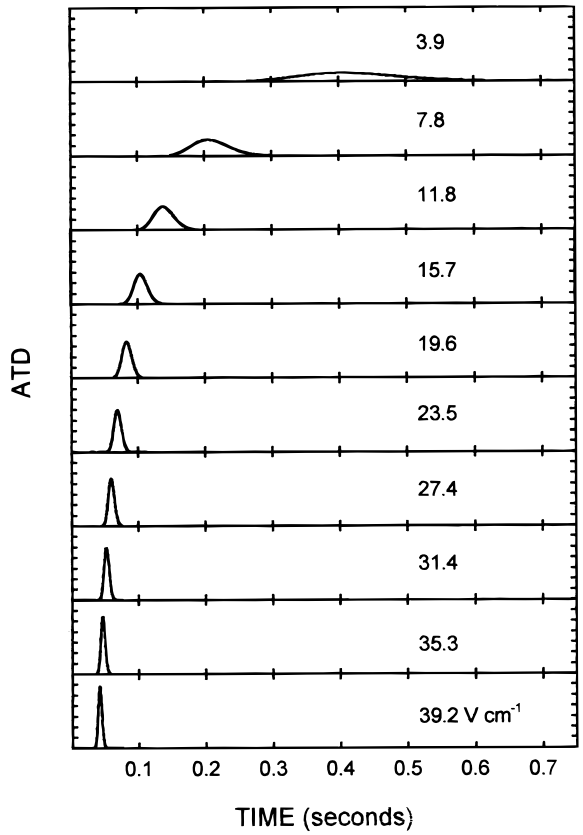

Figure 7. Calculation of the ion density in the nucleation zone as a function of time at different electric fields. The conditions used for the calculations correspond to the experimental conditions given in Figure 3. The ion mobility used in the calculation is $K = 0.60$ cm^2/Vs.

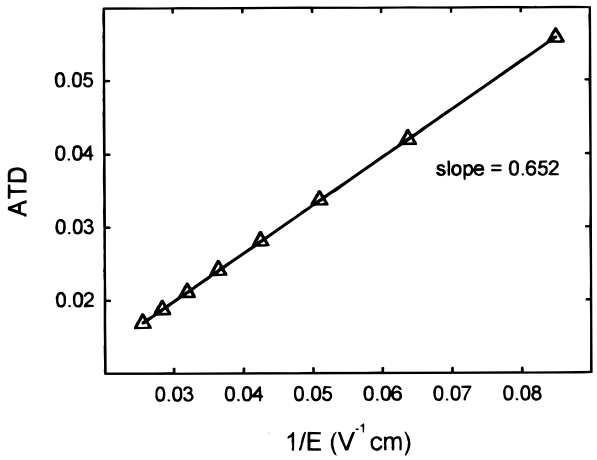

Figure 8. Calculated arrival time distribution as a function of 1/E (electric field) for the results shown in Figure 7.

The results are shown in Figure 7 for the toluene$^+$/methanol experiment. As seen in Figure 7, at smaller voltages the ion cloud at the nucleation zone is broader due to the longer time available for diffusion. Also, it is clear that the arrival time of the maximum ion density (ATD) is inversely proportional to the applied field as shown in Figure 8.

Using the calculated ion density, the TDC (total droplet count) can also be obtained. The TDC is the integral over the time of droplet detection of the scattered light signal caused by the nucleation event. Note that in pulsed ion nucleation experiments, the TDC can be measured directly and is the only parameter that can be used to reflect the rate of ion nucleation. In the approximation of geometrical optics, the TDC can be expressed

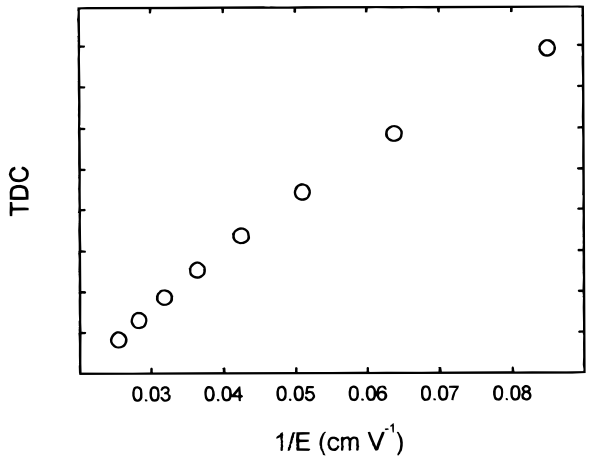

Figure 9. Calculated total droplet count as a function of $1/E$ (electric field) for the results shown in Figure 7.

as[41]

$$\mathrm{TDC} = \int_0^\infty n_\mathrm{d}(t) R(t)^2 \beta \mathrm{d}t \tag{14}$$

where $n_\mathrm{d}(t)$ is the number of droplets crossing the He−Ne laser beam at time t, R is the droplet radius, β is a constant that depends on the laser wavelength and optical properties of the droplets.[41]

In the nucleation experiments, the droplet radius depends on the vapor supersaturation, the total pressure, and the nature of the carrier gas.[22] When the thermodynamic conditions are constant throughout an experiment, the final droplet radius will be the same for all the droplets. Furthermore, because the optical properties of the nucleated droplets are the same, β will be a constant as well. Then the integrated scattered light intensity is primarily dependent on the number of droplets that are produced in the nucleation zone. When the above conditions are met, then the TDC will be dependent only on the concentration of ions in the nucleation zone and eq 14 may be rewritten as

$$\mathrm{TDC} \approx \int_0^\infty n_\mathrm{d}(t)\mathrm{d}t \propto \int_0^\infty n_\mathrm{i}(t)\mathrm{d}t \approx \frac{n_\mathrm{i}^* H}{KE} \tag{15}$$

where $n_\mathrm{i}(t)$ describes the time dependence of the ions in the nucleation zone, n_i^* is the maximum of ion density in nucleation zone, H is the width of nucleation zone. The dependence of the TDC on the electric field is obvious because the field defines the residence time of cluster ions in nucleation zone. The dependence of the TDC on the electrical field is of interest because it is directly related to the cluster ion mobility in the DCC nucleation experiments. Figure 9 displays the calculated TDC as a function of $1/E$ (applied field) for the ion distributions calculated in Figure 7. It is clear that the experimental dependence of the TDC on the electric field agrees well with the calculations. This indicates that the field dependence observed in these experiments results from the dependence of the ion distribution on the electric field. Therefore, it is evident that this observed field dependence does not result from any dependence of the ion nucleation kinetics on the electric field.

C. Comparison with Thomson's Model. It is interesting to relate the observed trend of decreasing cluster ion mobility with increasing vapor supersaturation to the predictions of Thomson's model for ion-induced nucleation.[29] In Thomson's model, the free energy of formation of a cluster of radius r_n around an ion of radius r_i and charge q is given by

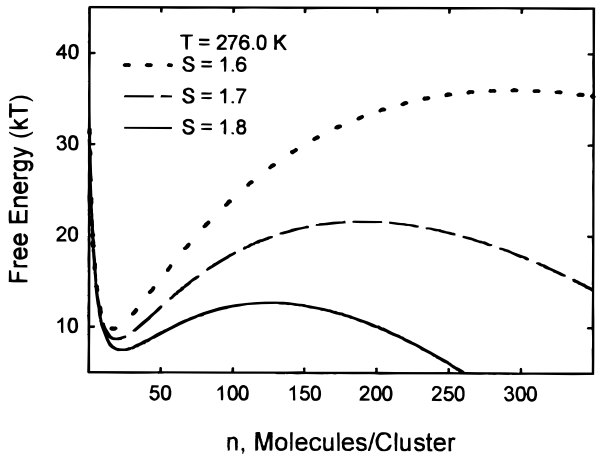

Figure 10. Free energy of formation as a function of cluster size according to Thomson's model for the ion-induced nucleation of methanol on toluene ions at $T = 276$ K and different methanol supersaturations as indicated.

$$\Phi(n) = -nk_\mathrm{B}T \ln S + 4\pi r_\mathrm{n}^2 \sigma + \frac{q^2}{8\pi\epsilon_0}\left(1 - \frac{1}{\epsilon}\right)\left(\frac{1}{r_\mathrm{n}} - \frac{1}{r_\mathrm{i}}\right) \tag{16}$$

where k_B is the Boltzmann constant, S is the vapor supersaturation ratio at temperature T, and σ and ϵ are surface tension and dielectric constant of the liquid, respectively. Figure 10 shows the free energy as a function of the number of molecules in the cluster for the ion-induced nucleation of methanol on toluene ions at $T = 274$ K and different supersaturations. The minimum in the free energy corresponds to the formation of the solvated cluster ion toluene$^+$(methanol)$_n$. Further growth occurs with an increase in free energy until the cluster reaches a size n^* (critical cluster or nucleus), after which, it grows with decreasing free energy to form a liquid droplet. It is clear that the size of the solvated cluster ion increases and the size of the critical cluster decreases with increasing the vapor supersaturation. Interestingly, at high enough supersaturation, the size of the solvated cluster ion coincides with the critical cluster size, and the barrier to ion nucleation disappears. Figure 11a shows the supersaturation dependence of the size of the solvated ion as predicted by Thomson's model, and Figure 11b illustrates the supersaturation dependence of the measured ion mobility. The similarity between the two trends is evident. Note that from the measured mobility, the size of the precritical clusters can be estimated through the mobility−size relationships, based on either the continuum model or on kinetic theories.[35,42] However, in the present study, we are only concerned with the trend of decreasing ion mobility with increasing the vapor supersaturation. The observation of this trend provides the first direct experimental evidence for the dependence of the size of the precritical clusters on the vapor supersaturation, as predicted by Thomson's model.

The differences between the current measurements and other ion mobility measurements should be emphasized. In the current experiments, the average mobility of the growing precritical clusters can be measured under typical nucleation conditions in which the vapor supersaturation, temperature, and partial pressures are well characterized. The vapor supersaturation in the drift region can be increased, and the average mobility of the growing clusters can be measured. This information is obtained simultaneously with the rate of ion-induced nucleation (number of nucleated droplets per cm^3 integrated over the time of the nucleation pulse for a given number of ions). The cluster ions are detected at the end of their drift distance (by light

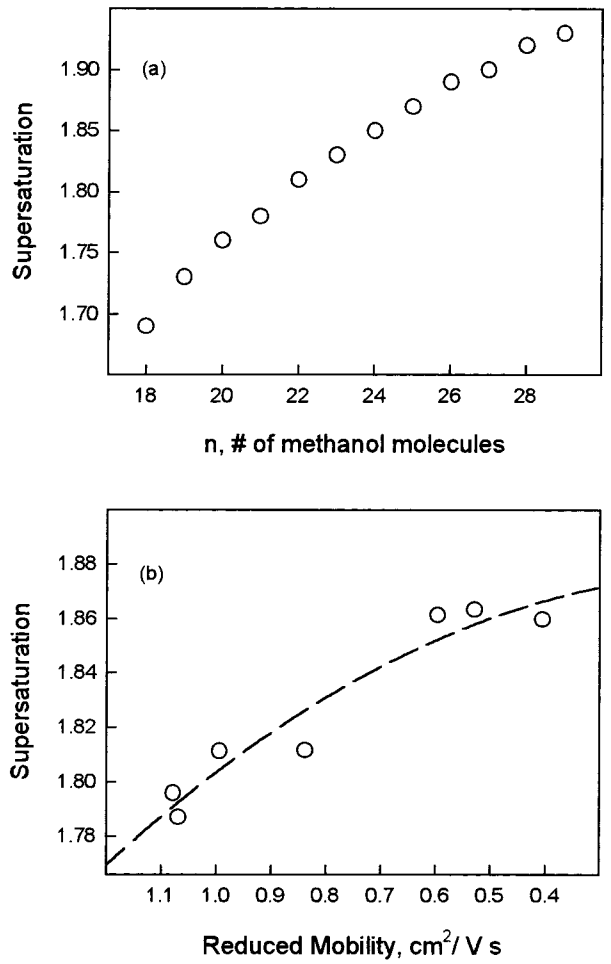

Figure 11. (a) Dependence of the size of the solvated cluster ion, toluene$^+$(methanol)$_n$, on the supersaturation of methanol vapor at $T =$ 276 K according to Thomson's model. (b) Dependence of the measured reduced mobility of the toluene$^+$(methanol)$_n$ precritical clusters on the supersaturation of methanol vapor within the temperature range of 274−276 K.

scattering from the nucleated droplets) as opposed to travelling from the drift tube to a mass spectrometer detector (orders of magnitude change in pressure) in typical ion mobility experiments.

4. Conclusions and Outlook

To conclude, we wish to point out that the method reported here provides the first experimental measurements of the ion mobility of precritical clusters in which the nucleating ions are identified under well-defined conditions of vapor supersaturation and temperature. The results verify the trend predicted by Thomson's model of increasing the size of the solvated cluster ion by increasing the vapor supersaturation. With this method, it is now possible to compare the mobility of precritical clusters containing positive or negative ions. This will provide the critical data necessary in order to resolve the long-standing question regarding the effect of the charge sign on the rate of ion-induced nucleation. Future work will address this subject.

Acknowledgment. The authors gratefully acknowledge support from NSF (Grant No. CHE 9816536) and NASA Microgravity Materials Science Program (Grant No. NAG8-1484).

References and Notes

(1) Abraham, F. F. *Homogeneous Nucleation Theory*; Academic Press: New York, 1974.

(2) Zettlemoyer, A. C., Ed. *Nucleation Phenomena*; Elsevier: Amsterdam, 1977.

(3) Senger, B.; Schaaf, P.; Corti, D. S.; Bowles, R.; Voegel, J. C.; Reiss, H. *J. Chem. Phys.* **1999**, *110*, 6421−6438.

(4) Oxtoby, D. W. *Acc. Chem. Res.* **1998**, *31*, 91.

(5) Reiss, H.; Marvin, D. C.; Heist, R. H. *J. Colloid and Interface Sci.* **1977**, *58*, 125.

(6) Reiss, H. *Science* **1987**, *238*, 1368.

(7) Wilson, C. T. R. *Philos. Trans. R. Soc. London Ser. A* **1897**, *189*, 265. Wilson, C. T. R. *Philos. Trans. R. Soc. London Ser. A* **1899**, *193*, 289. Note that C. T. R. Wilson (Cambridge, England) was awarded the Nobel prize in Physics in 1927 "for his method of making the paths of electrically charged particles visible by condensation of vapor".

(8) Rabeony, M.; Mirabel, P. *J. Chim. Phys.* **1986**, *83*, 219.

(9) Rabeony, H.; Mirabel, P. *J. Phys. Chem.* **1987**, *91*, 1815.

(10) Adachi, M.; Okuyama, K.; Seinfeld, J. H. *J. Aerosol Sci.* **1992**, *23*, 327.

(11) He, F.; Hopke, P. *J. Chem. Phys.* **1993**, *99*, 9972.

(12) Katz, J.; Fisk, J.; Charkarov, V. *J. Chem Phys.* **1994**, *101*, 2309.

(13) Seto, T.; Okuyama, K.; de Juan, L.; de la Mora, J. F. *J. Chem Phys.* **1997**, *107*, 1576.

(14) Arshadi, M.; Yamdagni, R.; Kebarle, P. *J. Phys. Chem.* **1970**, 74, 1474.

(15) Castleman, A. W., Jr.; Keesee, R. G. *Science*, **1988**, *241*, 36.

(16) Gouw de, J. A.; Ding, L. N.; Krishnamurthy, M.; Lee, H. S.; Anthony, E. B.; Bierbaum, V. M.; Leone, S. R. *J. Chem. Phys.* **1996**, *105*, 13 098.

(17) Bowers, M. T.; Marshall, A. G.; McLaffery, F. W. *J. Phys. Chem.* **1996**, *100*, 12 897

(18) Kane, D.; Daly, G. M.; El-Shall, M. S. *J. Phys. Chem.* **1995**, *99*, 7867.

(19) Kane, D.; El-Shall, M. S. *Chem. Phys. Lett.* **1996**, *259*, 482.

(20) Kane, D. B.; El-Shall, M. S. In *Nucleation and Atmospheric Aerosols*; Kulmala, M., Wagner, P. E., Eds; Elsevier Science Publishing: Amsterdam, 1996, 46.

(21) Kane, D.; Fisenko, S.; El-Shall, M. S. *Chem. Phys. Lett.* **1997**, *277*, 6.

(22) Kane, D.; Fisenko, S.; El-Shall, M. S. *Chem. Phys. Lett.* **1997**, *277*, 12.

(23) Kane, D. Application of Resonance Enhanced Multiphoton Ionization to the Study of Ion Nucleation in Supersaturated Vapors. Ph.D. Dissertation, Virginia Commonwealth University, Richmond, VA, 1997.

(24) Lubman, D. M.; Li, L.; Hager, J.; Wallace, S. C. In *Lasers and Mass Spectrometry*; D. M. Lubman, Ed.; Oxford University Press: Oxford, 1990.

(25) Jarrold, M. F. *J. Phys. Chem.* **1995**, *99*, 11.

(26) Clemmer, D. E.; Jarrold, M. F. *J. Am. Chem. Soc.* **1995**, *117*, 8841.

(27) Gouw de, J. A.; Krishnamurthy, M.; Leone, S. R. *J. Chem. Phys.* **1997**, *106*, 5937.

(28) Henderson, S. C.; Valentine, S. J.; Counterman, A. E.; Clemmer, D. E. *Anal. Chem.* **1999**, *71*, 291.

(29) Thomson, J. J.; Thomson, G. P. *Conduction of Electricity Through Gases*, 3rd ed.; Cambridge University: Cambridge, 1928; Vol. 1.

(30) Heist, R. H.; He, H. *J. Phys. Chem. Ref. Data* **1994**, *23*, 781.

(31) Kane, D.; El-Shall, M. S. *J. Chem. Phys.* **1996**, *105*, 7617.

(32) Breen, P. J.; Warren, J. A.; Bernstein, E. R.; Seeman, J. I. *J. Chem. Phys.* **1987**, *87*, 1917.

(33) Syage, J. A.; Al Adel, F.; Zewail, A. H. *Chem. Phys. Lett.* **1983,** *103*, 15.

(34) El-Shall, M. S.; Yu, Z. *J. Am. Chem. Soc.* **1996**, *118*, 13 058.

(35) McDaniel, E. W.; Mason, E. A. *The Mobility and Diffusion of Ions in Gases*; John Wiley & Sons: New York, 1973.

(36) Shumate, C.; St. Louis, R. H.; Hill, H. H., Jr. *J. Chromatogr.* **373**, *141*, 1986.

(37) Revercomb, H. E.; Mason, E. A. *Anal. Chem.* **1975**, *47*, 970.

(38) Kane, D.; Rusyniak, M.; El-Shall, M. S. In *Clusters and Nanostructure Interfaces*; Jena, P., Khanna, S. K., Rao, B. K., Eds.; World Scientific: New Jersey, 2000, 97.

(39) Raizer, Y. P. *The Physics of Gas Discharge*; Nauka: Moscow, 1987.

(40) Morse, P.; Feshbach, H. *Methods of Theoretical Physics*; McGraw-Hill: New York, 1953.

(41) Born, M.; Wolf, E. *Principles of Optics*; Pergamon: New York, 1980.

(42) Makela, J. M.; Riihela, M.; Ukkonen, A.; Jokinen, V., Keskinen, J. *J. Chem. Phys.* **1996**, *105*, 1562.